A review of phases, defects and machine learning in hybrid organic-inorganic perovskite solar cells

Bikal Khanal* and Madhav Prasad Ghimire*

* Central Department of Physics, Tribhuvan University, Kirtipur 44613, Kathmandu, Nepal.

Abstract: Hybrid organic-inorganic perovskite materials have been a field of keen interest in photovoltaic research community. Its improvement in efficiency over the last fifteen years has been the main motivation. Despite the development it has seen, there are two prevailing fundamental problems that need critical investigation. The first one is related to the formamidinium lead iodide ($FAPbI_3$) phase stability, whose photoactive phase happens to be thermodynamically metastable at room temperature. Another issue is non-radiative recombination caused by defects at grain boundaries and interfaces which lowers conversion efficiency of the devices. Literature from 2020 to 2026 seem to attempt to solve both the problems. We survey 51 studies that address these issues through tuning composition, integrating multidimensional architectures, additive and interface modification, and complementary DFT and machine learning approaches. Considering the computational side, DFT clarifies the effect of tolerance factor, octahedral connectivity and defects on the phase stability and defect tolerance. ML models accelerate screening of compositions, passivation techniques and device configurations by learning from the experimental and DFT data. The main idea is that phase stability, defects leading to recombination, and the data-driven methods dedicated to address them are not independent topics. This review organizes recent work around a single structure-defect-performance relationship, where experimental, DFT and ML findings converge or diverge. We conclude by discussing how this perspective can help us understand designing of perovskites that are not only efficient in laboratory but also structurally robust for long-term photovoltaic applications.

Keywords: Defect passivation; Hybrid perovskite; $FAPbI_3$; Machine learning; Phase stability; Structure-property.

Introduction

The energy demand in the world is increasing especially in the form of electricity, and we need it in a way that is renewable. Solar energy has proven to be a promising solution to this. For decades until now, silicon based solar cells have been our primary device for harvesting the solar energy. The challenge that we face in this field is that the Si (Silicon) based cells have reached their theoretical limit and the efficiency is not found satisfactory. Improving the efficiency in a cost effective manner is more difficult than ever [1,2]. This problem has motivated researchers to look for new class of materials that are cheaper and easier to make, can absorb light and convert it efficiently to electricity. Hybrid organic to inorganic solar cells have been one of the inorganic solar cells have been one of the most feasible

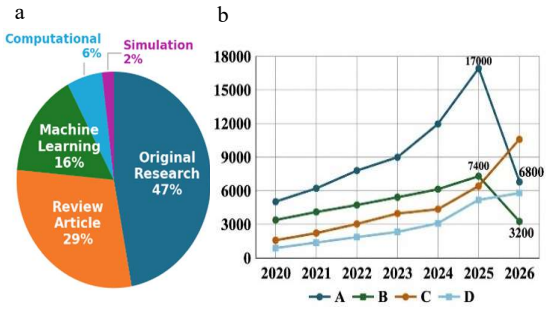

Figure 1: (a) Distribution of research articles type in this review work. (b) Research trend shown using number of published articles per year with results from following search keywords [Data retrieved from dimensions.ai]:

- **A. hybrid organic-inorganic solar cells**
- **B. hybrid organic-inorganic solar cells + machine learning**
- **C. hybrid organic-inorganic solar cells + DFT**
- **D. hybrid organic-inorganic solar cells + simulation**

Author for correspondence: Madhav Prasad Ghimire, Central Department of Physics, Tribhuvan University, Kathmandu, Nepal.
Email: madhav.ghimire@cdp.tu.edu.np; https://orcid.org/0000-0003-2783-4008
Received: 21 Apr, 2026; Received in revised form: 28 May, 2026; Accepted: 4 Jun, 2026.
Doi: https://doi.org/10.3126/sw.v19i19.95723

candidates in this context. They have shown improvement in efficiency from roughly 3% in the early 2010s to above 26% in 2025 as a single junction photovoltaic device [3,4]. This accelerated development stands as a motivating factor to explore more on this front.

This review is a thematic study compiled as a learning process to explore connection among key ideas across the field of perovskite solar cells. Citation tracing from established reviews and focused reading on selected themes are the primary methods for identifying articles for this review. This selection of the sources was driven by a motive to understand meaningful links and insights presented by the rapidly increasing number of articles, thus only a few of the enormous database are covered here. Searching for literature in this field for only last five years returned thousands of studies, and a student level review covering all of them would rather be diverging. This review explores and synthesizes conclusion limiting to only 51 sources. The selection procedure was based on four major criteria (i) directly addressing at least one of the topics: 'crystal structure and phase stability', 'defect chemistry and passivation', and 'machine learning assisted design', (ii) discussion on relation between structure and property, (iii) covering 2020-2026 period with a small inclusion of pre-2020 articles for establishing concepts and (iv) accessibility of reported results. Figure 1 presents the statistical overview of the published studies considered in this review. Here, Figure 1a illustrates the distribution of the article types using a pie-chart and Figure 1b depicts the annual number of published articles across different study categories related to the hybrid organic-inorganic perovskites solar cells. We have 24 articles (47%) based on original experimental research, 15 review articles (29%), 8 articles (16%) on machine learning with DFT, 3 studies (6%) on computational study and 1 paper (2%) based on simulation at device level covering a total of 51 sources. We do not aim to replace the expert reviews that exist on each of the themes presented here, those are more authoritative. We aim to connect the three approaches in a manner that is more comprehensible for someone starting to explore this area and show that phase stability, defect management and computational screening of materials are not separate problems but different expressions of the same underlying problem.

The ABX_3 based hybrid perovskites has A as an organic or small inorganic cation, B is a heavy metal, mostly Pb^{+2} and X is a halide (iodide, bromide or chloride). In this structure, PbX_6 is the component that is active in photo absorption and conversion. The A-site cation is lies inside the PbX_6 octahedra frame. Determination of stability is based on how well this cation fits in that framework which is described by Goldschmidt tolerance factor 't' [3–5]. In purview of hybrid organic inorganic perovskites two of the compounds are heavily focused, methylammonium lead iodide ($MAPbI_3$) and formamidinium lead iodide ($FAPbI_3$). $FAPbI_3$ has smaller bandgap of 1.48 eV and $MAPbI_3$ has that of 1.55 – 1.6 eV, making the former more suitable for absorption and photo current generation [1,2]. $FAPbI_3$ exists in two phases, α-phase and δ-phase. DFT calculations show that the band edges in the α-phase of $FAPbI_3$ is dominated by Pb-I states and the band gap is significantly reduced by the implementation of spin-orbit coupling (SoC). This also induces Rashba splitting contributing to longer carrier lifetime in FA-based cells [1]. The review further dives into the stability issues and target to establish why FA-based photovoltaic materials are preferred. Here, the interplay is between the light absorbing phase for active photovoltaic nature versus structural stability. The FA^+ cation is a bit too large to have ideal tolerance factor. Since the t value is a little beyond the stability range, the photoactive black α-phase is thermodynamically metastable and the ground state happens to be the yellow δ-phase [3,6,7]. The transition from metastable α to δ-phase disrupts the corner sharing octahedral network making the resulting bandgap unsuitable for photovoltaic application. Therefore, the challenge seen in the literature is to stabilize the α-phase without compromising on the optical properties. The later sections deals with various methods like mixing in Cs^+ and MA^+ to lower the t value [5,8], introducing 2D perovskites layers to lock the 3D phase [3,9,10], incorporating additives to increase barrier for the phase transition [3] and controlling the process of crystallization to obtain the desired phase [11–13]. All of these techniques come with some trade-off like widening bandgap, slow down charge transport [14,15],

introducing unwanted secondary phases [6] etc. Addressing this issue is what keeps the field active in research in current days and we do not have a definitive answer yet.

We are aware of the highest photo conversion efficiency for band gap of 1.48 eV is 33% as per Shockley-Queisser limit. The literature reveal that even when the α-phase is stabilized, efficiency is lowered by other factors and we have only about 26% PCE for $FAPbI_3$ [11,16]. This occurs due to non-radiative recombination, that are the places where electrons and holes recombine and lose their energy into heat and do not produce useful electrical work. The prime sites are grain boundaries, film surfaces and the interfaces of perovskite layers and charge transport layers. Passivation of the known defects happen to be the active area of study to gain better photovoltaic material. We found that Lewis base molecules coordinating to Pb^{+2}, halide donors for filling vacancies at X sites and 2D ammonium layers to block moisture are the two most explored techniques to suppress the defects [17–19]. Machine learning methods are helping this field to navigate the vast composition and processing space. They rely on descriptors based on composition like tolerance factors, ionic radii, bond angles to predict bandgaps and formation energies [20–22]. Later, ML focused on device level predictions like predicting PCE or mitigating the previously mentioned defects by identifying passivation molecules at interfaces have been explored [23]. More recently, delta-ML models have been deployed for bandgap with higher accuracy, graph neural networks (GNN) to directly encode compositional structure and predict structure-property relationships [22,24–26]. ML has become an important complementary tool in exploring perovskite photovoltaic materials, though a few challenges like limited data and accurate extrapolating remain [27].

The organization of this review is as follows. It moves from the basic structural and electronic features of hybrid perovskites to the prime challenges. The challenges include limited device performance, defects, phase stability and issues at the interface of different layers . The later sections discuss on how compositional modifications, controlling dimensions using computational approach address them. This leads to machine learning and device level simulation discussion revealing them as the major tool in screening and performance prediction. The goal is to arrive at a

Table 1: Effect of Goldschmidt's t value on structure and performance of some perovskite photovoltaic materials.

Composition	t value	Phase stability	E_g(eV)	PCE %	Inference	Reference
$MAPbI_3$	0.912	Moderate	1.55	25.5	t<1 causes A-site mismatch and tetragonal distortion occurs	1,2,4
$FAPbI_3$	0.987	Poor	1.48	26.1	delta phase is favored thermodynamically	3,4,6,7
$CsPbI_3$	0.805	Poor	1.73	20.2	t less than 0.81 enhances octahedral tilting and stabilizes in non-perovskite delta phase	25,28
$CsPbBr_3$	0.82	Good	2.3	10.6	has wide bandgap	
$FA_{0.83}Cs_{0.17}PbI_3$	0.97	Good	1.51	24.8	Cs substitution reduces transition to delta-phase	5,8
$CsFAMAPbI_{2.55}Br_{0.45}$	0.95	Excellent	1.6	25.7	Overall stability is good, but t value is observed to vary	
$MASnI_3$	0.91	Very poor	1.3	13.4	Sn2+ oxidizes to Sn4+	29,30
$FASnI_3$	1.02	Poor	1.41	14.6	t greater than 1 causes off-centering and structural instability	
$CsSnI_3$	0.795	Very poor	1.3	8.9	t less than 0.80 produces strong octahedral tilting and rapid degradation of the 3D network	
$MAPbI_3$_PEA	0.91	Excellent	1.55	24.5	needs proper passivation at 2D/3D interface for stability	14–16

comprehensive link among these topics for the readers following this field with computation, theory or experiments.

Why is perovskite a preferred structure?

A perovskite structure (ABX_3) is a network of corner-sharing MX_6 octahedra, structure shown in Figure 2. Here, M is typically a heavy metal like Lead (Pb) or Tin (Sn). This structure is repeatedly reported to produce bandgaps in the ideal range, good optical absorption and electronic features with minimum disruption from defects for photovoltaic applications. ABX_3 structure permits for substitutions on the A and X sites, which can tune lattice parameters, octahedral tilts and M-X-M bond angles. These structural variations directly affect bandgap, carrier effective masses and defect formation energies. To understand phase formation and stability, Goldschmidt tolerance factor, calculated as $t = \frac{r_A + r_X}{\sqrt{2}(r_B + r_X)}$ and octahedral factor, $\mu = \frac{r_B}{r_X}$, are used [4,8]. These geometrical parameters basically explain how well the A cation accommodates inside the BX_6 octahedra. Values apart from 1 indicate distortion from the perfect cubic perovskite structure. If t > 1, hexagonal phase is favored and for t < 1, orthorhombic phase is favored. In case of α-$FAPbI_3$, the tolerance factor is close to 1, about 1.03, meaning the perovskite structures is stable but sits at the upper edge of the tolerance window[4,6,7]. However, in case of $MAPbI_3$, the tolerance factor is slightly lower, about 0.96. This gives an insight on how the geometry can be altered by choice of cations which in turn change the property like bandgap, defect tolerance and carrier transport characteristics. A summary of t value with its effect on structure and material performance is presented in Table 1.

Byranvand *et al.* reviewed mixed cation at A-site in thin films and colloidal nanocrystals and showed that minor substitution of Cs^+ into FA/MA based lead halides can improve the tolerance factor to bring it closer to unity [8]. These geometric arguments for structurally complex hybrid systems underlines the feasibility to improve photovoltaic performance of perovskites which makes the ABX_3 structure one of the best family for solar cell materials.

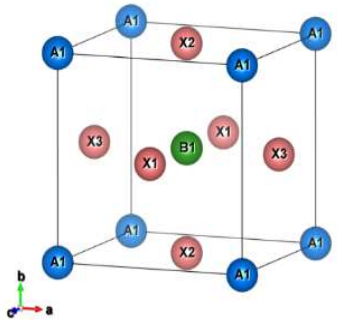

Figure 2: Schematic of a cubic perovskite structure (ABX_3) with B atom at the body center.

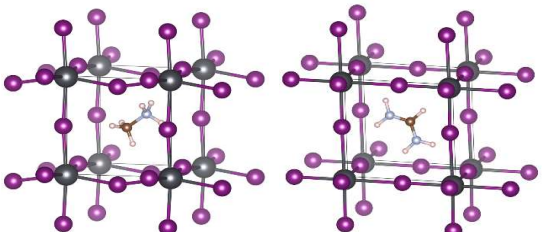

Figure 3: Structure of $MAPbI_3$ (left) and $FAPbI_3$ (right) with A-site organic cation at the body center.

$MAPbI_3$, $FAPbI_3$, and mixed A-site cations

Within ABX_3 lattice, the mixing of A-site cations serve as the primary variable to map structural stability with optimal electronic features. Figure 3 shows the MA^+ and FA^+ cations at A-site in the ABX_3 structure. FAPbI3 has a desirable bandgap of 1.48 eV and is a preferred material for absorption. But the Goldschmidt's t factor of FA^+ is near the upper edge in stability window making the α-phase susceptible to transform into the δ-phase, which is a non-perovskite form, under thermal and environmental stress [6,7].Zheng *et al.* reported that this α-phase can be kept stable by making the formamidinium ion fit better within the lead iodide frame by A-site alloying with smaller cations like methylammonium (MA^+) or Cs^+, surface functionalization using long-chain ammonium groups, strain regulation via substrate interaction etc [6]. Wang *et al.* supported this argument by classifying stabilization techniques into chloride based additives, pseudo-halide anion substitution (such as SCN^-, formate) and ionic liquid engineering revealing in each case that the crystallinity is improved, anion vacancy is reduced and the transition from α- to δ-phase is suppressed [7]. We already noticed that the MA^+ sits

more comfortably in case of the tolerance factor. However, the smaller MA^+ cation and the interaction of the PbI_6 frame with its hydrogen bonding results in faster chemical and thermal degradation under external environmental conditions. Such degradation is undesirable in practical use. Byranyand *et al.* showed that low concentration of MA^+ and higher concentration of FA/Cs compositions can optimize the tolerance factor, reduce octahedral tilting and suppress the phase change [6,8]. In a first principles study by Sa *et al.,* tolerance factor between 0.84 and 0.87 was found with confirmation of thermodynamic stability and direct bandgaps in range 1.0 – 1.3 eV using density functional theory (DFT) approach with hybrid HSE06 functional and van der Waals correction in a mixed-cation mixed-metal system, $MA_{1-x}Cs_xPb_{0.25}Sn_{0.75}I_3$ [21]. This DFT result agreed well with experimental practice of modification of A-site cation to rather engineer PbI_6 structure than just changing chemical composition.

Band structure, spin-orbit coupling and optical response

Perovskite framework is known to have direct bandgap at the Brillouin zone (BZ) center with strong optical absorption. The valence band maximum (VBM) is featured mainly by antibonding Pb-6s – X-p states whereas the conduction band minimum (CBM) has primary contributions from Pb-6p orbitals. The antibonding nature of VBM coming from the hybridization of Pb-6s and halide p orbitals makes most of the intrinsic point-defect states. This includes halide vacancies to adopt shallow energy positions near the band edges hence suppressing non-radiative recombination resulting in characteristic defect tolerance of hybrid lead halide perovskites[21,22]. Li *et al.* reported the usage of this defect-tolerant electronic structure by passivating agents. The study showed that Lewis acid or base functional groups can interact with Pb^{2+} and vacant halide sites that arise from the above-mentioned antibonding character of VBM[19]. Gao *et al.* found that the charged defects can be neutralized using quaternary ammonium halide-based passivators. This results in relating electronic structure of functional group and its interaction with the perovskite lattice [17].

Preference of hybrid over pure inorganic perovskites for PV applications

The resulting PV properties of organic-inorganic hybrid lead halide perovskites must be acknowledged in context of wider family of the similar chemical formula. ABX_3 framework is common to a diverse set of compounds ranging from fully inorganic $CsPbI_3$ with Sn- and Ge-substituted systems to hybrid MA^+/FA^+ lead iodide systems. A systematic comparison of each type against the hybrid system reveals the superiority of the latter one is due to the desirable alignment of structural, electronic and photovoltaic properties. In a pure Cs based system, the substitution of A-site Cs^+ (r = 1.67 Å) by MA^+ resulted in volatilization under high temperature represented one of the major degradation in hybrid material [29]. $CsPbI_3$ being the most studied candidate is thermally stable up to 310ºC. In this perovskite the Cs^+ ion lowers the Goldschmidt's tolerance factor to approximately 0.81 due to its smaller radius. This is well below the perfect cubic window of 0.9 – 1.0 indicating a strong thermodynamic favor towards the non-perovskite orthorhombic yellow phase at room temperature[25]. Figure 4 shows how organic cation-based perovskites fall in stable group as per the tolerance factor t.

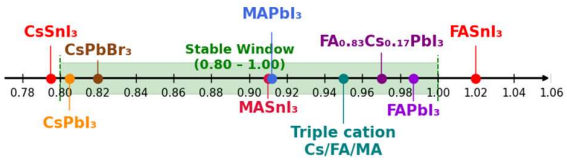

Figure 4: Number line of Goldschmidt's t-values with position of perovskites showing their stability.

The black α-$CsPbI_3$, which is photoactive, has a bandgap of 1.73 eV and lies above Shockley-Queisser limit for single junction, 1.34 eV. On substituting halide with Br^- increases the bandgap further making $CsPbX_3$ more suitable candidate for a wide-bandgap layer in tandem configurations than a single junction absorber. Apart from the bandgap, this purely inorganic compound also suppresses the soft-phonon dynamics that is responsible for large-polaron formation thereby having short carrier lifetimes, unlike hybrid systems[28].

The replacement of Pb^{2+} by Sn^{2+} (r = 1.35 Å) shrinks the

octahedral cage of PbI_6 reducing the Pb-I-Pb bond angle that causes shift in bandgap of $FASnI_3$ to about 1.41 eV. This being near ideal value for single junction photovoltaics, becomes the primary motivation for obtaining lead-free compositions [30]. Under ambient conditions, Sn^{2+} easily oxidizes to Sn^{4+} introducing a high concentration of deeper hole-trap states and results in self-p-doping. The lifetime of minority carriers is shortened by the new carrier density by several orders of magnitude compared to Pb^{2+} system. This causes irreversible degradation of the material. As of 2026, Sn based power conversion efficiencies (PCE) remains below that of Pb based PCE even after suppressing the oxidation through additives for reduction or antioxidant co-solvents. Germanium based perovskites also suffer from similar oxidation, $Ge^{2+} \rightarrow Ge^{4+}$ and thus has structural instabilities [29,30].

The choice of MA^+/FA^+ lead iodide systems at this point of PV material development is based on several simultaneous criteria that none of the pure inorganic or lead-free compositions meet together. Firstly, the FA^+ ion has ionic radius of 2.53 Å that brings the tolerance factor of $FAPbI_3$ near unity that ensures cubic phase and a bandgap of 1.48 eV ensures close to Shockley-Queisser optimum for a single-junction device [25]. Next, Dutta *et al.* confirms that the varying orientations of the organic cation in PbI_6 frame provides this octahedra frame a soft acoustic phonon mode enabling large polaron generation and suppresses non-radiative recombination unlike Cs based system that has a fixed position of the cation [31]. Lastly, Zhao *et al.* and Jiang *et al.* propose that the lower crystallization enthalpy of the hybrid phase, although makes it thermodynamically weak, enables these crystals to form easily at low temperatures and allows atoms/ions to move freely helping the grains merge and grow larger that improves charge transport [32,33]. It is also of the interest to acknowledge that the tandem systems partially address the bandgap limitation of inorganic perovskites with wide bandgap by pairing them with bottom cells having lower gap. This has been demonstrated in a two-terminal perovskite-perovskite device with 1.8 eV $CsPb_2Br_5$ as the bottom cell for wide gap top cells producing 31.13% PCE [34]. Nevertheless, in 2020 – 2026 window, the organic- inorganic hybrid system, specifically with FA^+, Pb based and mixed cations systems remain dominant in terms of performance with respectable structure-property relationship. Improvement of PCE of FA based compounds in this short duration can be observed in Figure 5. The following sections in this review therefore adopt $FAPbI_3$ and its mixed-cation derivatives as the reference system for discussion.

Phase stability: challenge and ways to meet it

The α – δ issue in $FAPbI_3$

The previous section establishes the argument on tolerance factor for $FAPbI_3$ that the phase producing near ideal

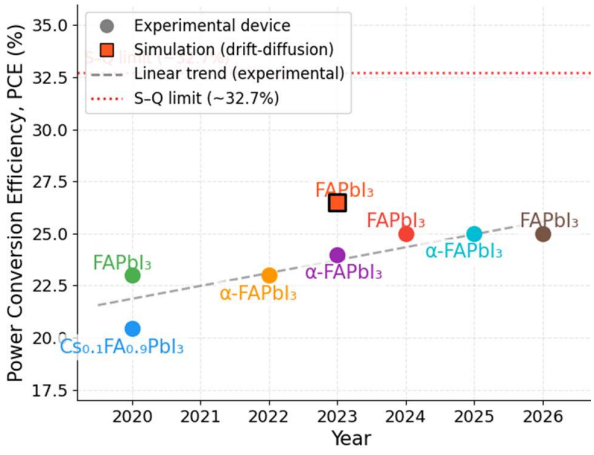

Figure 5: Trend of PCE improvement in hybrid organic-inorganic perovskite solar cells from 2020 to 2026.

bandgap (α) is thermodynamically less stable than the other competing phase (δ) at room temperature. The δ polymorph is a one-dimensional hexagonal structure with face-sharing PbI_6 octahedra and a photovoltaically undesirable bandgap of 2.4 eV. This is the reported ground state [33]. The metastable α phase must be kinetically trapped instead of growing into thermodynamic equilibrium because it will end up in its favorable ground state otherwise. Here, the iodide vacancies are the chief reason for speeding up this transition. Dutta *et al.* performed machine-learned force field (MLFF) calculations to confirm that increasing the iodide vacancies concentration reduces the activation barrier for the unwanted transition into δ phase by disturbing the electrostatic interactions between Pb^{+2} and I^- ions in the 3D lattice[31]. This disrupts the structural

integration by weakening the Coulomb attractions along the Pb-I-Pb links. Environmental factors such as temperature, moisture and illumination with light of lower energy than bandgap further lowers the barrier in manners like thermal activation, protonation of the I^- cage, adding iodide vacancies respectively. To revert from the δ phase to α phase, it requires annealing above 150ºC, making it impractical.

Optimizing composition to stabilize the phase

The fact that composition defines the tolerance factor has been well established in the previous sections. Now the first technique is to refine A-site mixture. In the second section, Cs^+ addition and MA^+ reduction was shown to improve the tolerance factor towards unity. We did not discuss the mechanism of grain boundary through which the cations interact. Cs^+ is a smaller ion than FA^+, so it drifts to grain boundaries under higher temperature. The grain boundary often has a thin, disordered amorphous layer which becomes thermally more robust because of Cs addition. By this process, the mobility of halide and A-site ions are suppressed along the grain boundary thereby preventing structural degradation. This function of the smaller Cs^+ ion is another contribution besides optimizing the Goldschmidt tolerance factor[8]. In case of MA^+ cation in A-site mixture, the residual MA^+ after MACl evaporation, although present in small fraction, at grain boundaries affects the structural stability of the device and also causes low-energy decomposition as $MA^+ + I \rightarrow MAI(gas) + Pb^0$ under continued illumination [32]. This suggests that precise stoichiometric estimation of MACl loading is necessary to do just grain growth and morphology but not so much that it triggers degradation at grain boundaries. We can note that mixed halide system has some instability issues, partial substitution of Br^- in I^- site increases the bandgap for tandem system but the mixed halide lattice suffers light induced halide segregation driven by localized strain fields. This issue is not addressed by the tolerance factor adjustment and requires geometric confinement. The next section deals with this.

Degradation effects of moisture, heat and light

After establishing the phase transition mechanism, a need for understanding of degradation processes arises. This can be classified into two types – intrinsic and extrinsic depending on whether the material's degradation cause is based on factors outside the lattice or not. In intrinsic type, degradation occurs purely from inside the perovskite. Iodide vacancies prefer to move along (110) paths with low energy barriers; hence they are highly mobile under operating conditions. This motion causes J-V hysteresis, halide redistribution and reduction of Pb^{2+} to Pb^0. Also, the previously mentioned phase transition is intrinsic. These two processes interact and was found that the iodide vacancy motion accelerates α → δ transition by lowering the energy barrier. As more δ phase forms and grains convert, new grain boundary areas providing additional pathways and vulnerable surface for any external factors (moisture, oxygen, etc.) thereby compounding degradation[26]. On the other hand, extrinsic pathways require environmental factors. Moisture interacts with the hydrogen bonding of A-X sites introducing H in X locations resulting in release of the organic cation as a volatile ion. O_2^- is generated by molecular oxygen under illumination by interacting with holes. O_2^- then deprotonates the A cation. UV rays carry sufficient energy to ionize I^- and releasing I_2 and obtaining Pb^0 without water or oxygen[29].

Multi-scale defect and interface management in perovskite solar cells

As of 2026 a common perspective in the literature can be observed that the stabilization techniques discussed previously are necessary but not individually sufficient. Devices with single treatment such as composition modification, adding additives, or encapsulating the material show clear improvement in stability. But this has not been yet commercially feasible due to low lifetime. Jiang *et al.* calls this limitation as a multi-dimensional regulation problem in which bulk crystal quality, grain boundary issues and absorber – interface passivation demand coupled improvisation and not isolated treatment of each defect. When all the three techniques were implemented in n-i-p $FAPbI_3$, it was reported that the real life PCE obtained was above 25% along with T_{80} lifetime exceeding 1000 h under continuous AM1.5G illumination

at environmental temperature of 65 ºC [33]. This result has never been met till date with just a single intervention.

2D, 3D and hybrid perovskite structures for photovoltaics

The discussion from the previous section on stability extends here as engineering the dimensionality addressing the connectivity of the inorganic octahedra (MX_6) cage could be modified to balance charge transport and structural stability.

This section deals with the modification of the MX_6 octahedra framework that could have 2D/3D or hybrid dimensionality to gain better balance of charge transport and structural robustness [35,36]. On moving from a 3D corner shared octahedral framework to a layered (2D) or chain-like (1D) introduces confinement of carriers within thin inorganic slabs separated by wide bandgap organic ions. These low dimensional structures are robust to moisture, oxygen and thermal stress than the 3D systems. In 2D since the inorganic and organic layers have distinct dielectric properties, they modify Coulomb interactions and excitonic properties. This process raises exciton binding energies and make the carrier motion difficult out of the plane i.e. perpendicular to the layers. Therefore, a 3D $FAPbI_3$ cannot be fully replaced by a lower dimensional equivalent just for higher efficiency because of limitations in transport and exciton issues. These layers are but auxiliary to stabilize the 3D bulk [29,32].

Dimensional structure and charge transport in halide perovskites

The spectrum of dimensionality spans 3D corner shared networks, layered quasi 2D phases and electronically confined 1D and also 0D systems[32,36]. The discussed $FAPbI_3$ is a 3D structure that provides a network of octahedra in all spatial directions. This makes it preferable system for longer diffusion length and efficient vertical transport [5,32]. Zhao *et al.* [32] discuss the introduction of layered Ruddlesden-Popper (RP), Dion-Jacobson (DJ) and alternating cation in the interlayer (ACI) perovskites disrupt the 3D frame by inserting organic layer cations between the inorganic slabs. This forms multiple quantum well like structures. Since the connectivity of the octahedra frames is now reduced, it was shown to improve moisture resistance and structural degradation but at the cost of higher exciton binding energy and hinders vertical transport compared to 3D systems. In this sense we see how 2D layers are valuable when they are used selectively especially at the surfaces and interfaces rather than in the entire bulk of the material [31].

In the layered group, Ruddlesden-Popper (**RP**) perovskites have two monovalent layer cations separating the neighboring inorganic slabs. This creates a van der Waals gap with weaker interlayer coupling. In case of Dion-Jacobson (**DJ**) perovskites, they use a single divalent layer that bridges the neighboring inorganic slabs. Here the Ruddlesden-Popper phases exhibit higher exciton binding energies (a few hundred meV) and strongly confined carriers, whereas Dion-Jacobson phases show stronger electronic coupling between layers, lower exciton binding energies and better transport as the van der Walls gap is absent. Alternating cation in the interlayer (**ACI**) phases, representing an intermediate structure, has tunable dielectric confinement and interlayer interactions [32]. Some lower dimensional perovskites are still in their early stage of study such as 1D/3D and 0D/3D systems use chain or cluster like formation to passivate trap states and brings stability to the 3D phase [36].

Organic cation as a variable for structural design

After dimensionality is lowered, the A site cation becomes a variable to control structure directly rather than being just a passive additive. The interlayer distance, degree of inorganic slab distortion and the strength of electronic coupling across the organic barrier is determined by the size, valence, rigidity functional groups and packing of the organic cation [16]. This shows the importance of this spacer cation selection, here it is commonly seen how effectively it protects and regulates $FAPbI_3$ based 3d, than, whether it can replace that phase [36]. A properly chosen spacer cation can help form ultrathin 2D perovskite layers at the outer surface of a 3D absorber where the under coordinated sites are passivated and lattice distortions are suppressed while keeping the bulk of $FAPbI_3$ for proper charge transport [22,31].

2D and 3D mixed structures

The central message of the dimensionality of the materials is that it naturally results in composite devices including both 2D and 3D structures. Here only a small portion of low dimensional phase is introduced to a 3D absorber. Thote *et al.* demonstrated that on a $FAPbI_3$ film, deposit of phenethylammonium based 2D layer at grain boundary strengthens phase stability and controls moisture induced degradation[37]. This result established a trend that the 3D phase remains the primary light absorber and charge transport entity while the 2D phase would act as a protective layer, suppressing defects and avoiding degradation[37,38].

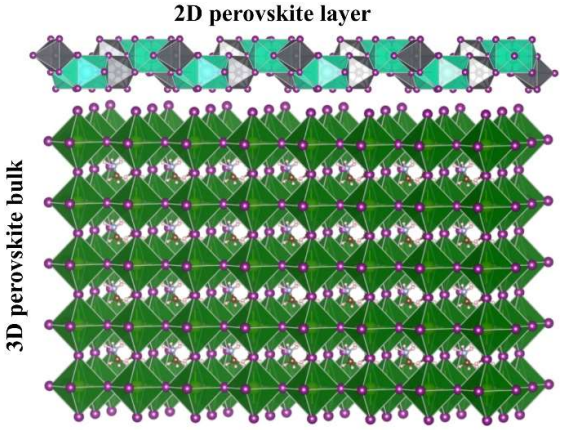

Figure 6: A schematic of 2D layer on top of 3D perovskite photovoltaic material.

A 2D layer sitting on top of 3D bulk is shown in Figure 6. This formed the basis for study in 2020 with some variations adopted for the location of the 2D components. Hu *et al.* demonstrated that dispersing PEA_2PbI_4 nanosheets inside $Cs_{0.1}FA_{0.9}PbI_3$ lattice, a small fraction of the 2D nanosheets assist in locking the α phase along with reduction in trap sites number and elongating carrier lifetime. This resulted in photovoltaic devices of up to 20.44% PCE with 82% of initial efficiency even after 800 hours of use [10]. Liu *et al.* synthesized a 2D $IBA_2FAPb_2I_7$ layer on top of α-$FAPbI_3$ film through two step annealing. Confirming via GIWAXS and TEM, the authors claim that α to δ transition was suppressed with passivation of surface defects. This study led to yield devices close to 23% PCE with 85% initial efficiency after 500h of 1-sun illumination at 80ºC. Another study exposed that post treatment of 3D absorbers with organic ammonium salts results in 2D-3D heterostructure where the carriers flow from large energy gapped 2D layer into the 3D bulk. V_{OC} was observed to improve with better performance under environmental stress [39].

A review work by Ge *et al.* compiled these results and provided a comprehensive framework concluding that focusing on 2D/3D multidimensional structures can protect from moisture and gain stability due to high formation energy of 2D perovskites while maintaining charge transport and light absorption of the 3D bulk. A-site cation composition acts as the prime design parameter covering both phase stability and recombination at the interface of these layers [40]. Despite the mentioned developments, a key question prevails – could these 2D phases stabilize the pure α-$FAPbI_3$ without heavy mixing of the A site cation. On depositing a thin 2D layer on top of the α-$FAPbI_3$ film to form a 2D-3D heterostructure suppressed the α to δ transition under moisture and thermal stress. This also maintained bandgap of 1.48 eV. Therefore, without heavy cation alloying, the stability was gained [41]. This solution comprises of some risk that was later discovered by Liu *et al.* in 2025. The study provides a clarification on benefits as well as risks of incorporating the 2D layer. With the help of GIWAXS and GIXRD, the authors showed that long chain alkylamine ligands disrupt the corner sharing PbI_6 connection at the surface of the 3D film. This creates 2D perovskites layer having lower Young's modulus than the 3D component causing elastic relaxation of in-plane strain as confirmed by high Miller index reflections showing negative 2θ shifts [15]. Chen and Jiang *et al.* implemented a new strategy by forming a layer of localized 2D-3D heterojunction confined only to the deeper interface. This was achieved by exploiting Lewis acid-base interactions between ammonium ligands and a hole selective monolayer. This confirms the presence and localization of the 2D phase at this interface as shown by results of GIWAXS and KPFM. Such layer reduced defect density at the deeper interface and enhanced transport property of the bulk. Implementing this strategy the achieved band gaps of the devices are 1.68, 1.79 and 1.85 eV with photovoltages of 1.30, 1.38 and 1.42 V. All of the devices were reported to achieve open-circuit voltages of more than 90% of the

thermodynamic Shockley-Queisser limit. This indicates that non-radiative recombination losses at the deeper interface are avoided largely[33,42].

n-value and structural distinction in DJ and RP phases

In this context, the n-value refers to the count of how many inorganic octahedra layers sit in one well between spacer cations and layered perovskite. For n = 1, a single inorganic layer sits between the spacers. For larger n (=2, 3, 4 …) we get thicker organic layers and weaker exciton binding compared to that of lower n values [16]. It is clear that the n value is a parameter to tune from better stability to better transport feature. In case of $FAPbI_3$, the appropriate n value depends on whether the component with lower dimension acts as a bulk modifier or as a thin, localized surface.

Beyond this, we have RP and DJ structural phases. The DJ divalent layer has stronger interlayer bonding that connects interlayer octahedra removing the van der Waals gap than the monovalent RP equivalent [43]. Here, lower n-values resulted stronger quantum confinement but limited charge transport through 2d layer, and higher n-values gave higher transport with comparatively weaker confinement.

On optimizing the n value, devices with 25.56% of PCE were obtained with better stability against moisture and thermal stress. This demonstrated DJ phase resolved both transport and stability issues that constrained RP ones [43]. We are also provided with a broader benchmarking by Shen *et al.* which identified DJ type 2D structures performed better than the RP phases in interfacial stability due to

Table 2: A summary of comparison of ML methods observed in various published works highlighting their specified tasks and challenges faced.

ML Method	Task performed by the ML model	Input Descriptors needed	Challenge observed
General ML workflow[20]	Stability & bandgap prediction of cubic phase	Goldschmidt tolerance factor, octahedral factor, ionic radii, electronegativity	Training data are limited and biased causing lower quality of prediction accuracy outside the data range.
DFT + supervised ML (high-throughput screening)[22]	Compositional screening of ABX_3 and double perovskites	Tolerance factor, ionic radii, electronegativity difference, formation energy	Model is not very accurate on test data
Delta-ML [22]	Prediction of high-accuracy bandgap	Base ML prediction + small high-fidelity DFT correction dataset	Requires reliable base model and small DFT correction dataset
Drift-diffusion simulation[45]	Prediction of device-output like PCE, V_{OC}, $J_{SC,}$ FF etc.	Defect density, layer thickness, doping concentration, energy level alignment	This model cannot propose/predict new compositions
Molecular descriptor-based ML[23]	Ranking passivation molecule for p-i-n cells	Lewis acid-base character, H-bonding capacity, functional group identity	Requires prior experimental passivation data for training
Active learning + Bayesian optimization[46]	Designing Defect and interface linking to simulation and experiment	Defect chemistry and interfacial data	Current models lack grain boundary and surface state descriptors
ML + automated synthesis + high-throughput characterization[46]	Pre-filtering of promising candidates	Composition, device architecture, transport layer descriptors	Synthesis-dependent phases not captured by descriptors
Supervised ML (RF, GBT, neural network)[47]	Prediction of Bandgap & PCE	Tolerance factor, ionic radii, electronegativity, formation energy	Cannot capture processing-dependent microstructure
Graph Neural Network (GNN)[24]	PCE prediction directly from compositional graph	Atoms, bonds, angles encoded as graph nodes and edges	limited perovskite training sets available
Machine-learned force field (MLFF)[26]	Prediction of ion migration path in halide perovskites	Atomic forces calculated from DFT along migration paths	Requires large DFT dataset for reliable force field training.

.

removal of the van der Waals gap [44]

Computational and Machine Learning Methods to Perovskite Design

First principles as a foundational study for structural and electronic features

First principles as a foundational study for structural and electronic features Electronic structure of hybrid perovskites study basically covers most of the data driven approaches for this field of research. Wang *et al.* used density functional theory (DFT) to study cubic α-$FAPbI_3$ with PBE, PBE + vdW, HSE06 and GW functionals with and without spin-orbit coupling (SoC). They found that the orientation of FA^+ cation along (111) (ground state) at a low temperature and disordered alignment along (100) at room temperature had some difference on lattice parameters. But, the nature of band edges remains untouched by the FA^+ orientation which is clearly governed by the Pb-I orbital interactions. The inclusion of SoC lowered the bandgap by almost 1 eV compared to the scalar-relativistic PBE and also showed Rasbha effect lowering the effective mass. This provided a first principles view of long carrier lifetime and high photocurrent density as observed in experiments too. The study revealed that the α-$FAPbI_3$ has narrower bandgap and lower effective masses compared to $MAPbI_3$. This forms the background of why FA based devices show higher J_{SC} than the MA based ones [1]. The experimental evidence of this was given by Wei *et al.* [2]. The DFT based results showed near ideal bandgap of 1.48 eV, low effective mass, high absorption coefficients and SoC enabled Rasbha splitting. This study covered most of the prime areas in this field forming a foundation for all other data-driven approaches like machine learning.

Machine Learning (ML) approach for perovskite solar cells

A-site accessibility for mixing cations, B-site choice of metal, X-site composition of halides, dimensionality motivated the deployment of high throughput ML techniques as the use of DFT or experiments would be too demanding to explore the vast space of composition and other features [47]. A review by Liu *et al.* (2023) on ML models for perovskite addressed bandgap and power conversion efficiency (PCE) prediction, processing pipelines to handle large experimental perovskite solar cells datasets implementing feature engineering for encoding composition, device architecture and transport layer labeling. It was demonstrated that ML models trained on pre-processed datasets can predict accurate bandgap and PCE, which is also was found to be consistent with Shockley-Queisser framework. This helped to identify compositions related to high performances. It was concluded that physical descriptors are more reliable compared to empirical or black box feature to gain good predictions and avoid overfitting [47]. Tao *et al.* reviewed a general ML workflow to address perovskite based materials discovery. The article informs us about descriptors construction, model training, validation and usage, demonstrating structural descriptors like Goldschmidt tolerance factor, octahedral factors, ionic radii and electronegativities improve the predictions of stability and bandgap of cubic phase hybrid perovskites [20]. This study showed that with proper data and descriptors we can reduce reliance on expensive DFT calculations by utilizing ML approach [20]. In context of ML method, the central challenge that has prevailed from beginning is the data quality, sparsity and biasness. Kumar *et al.* reviewed active learning and Bayesian optimization methods that connect simulation, experiments and ML models to identify the need for incorporation of defect chemistry and interfacial data to form models of next generation [46]. Various ML approaches are summarized in Table 2 as per their implementation.

ML assisted screening of composition based on desired features

Identification of new or underexplored compositions with suitable bandgaps for specific photovoltaic usage is one of the most direct and useful applications of machine learning (ML) [48]. Chen *et al.* integrated high throughput DFT calculations and supervised ML models to screen a large chemical space of ABX_3 and double hybrid organic inorganic perovskites. They used physical descriptors like tolerance factors, ionic radii, electronegativity differences

and formation energies and the model efficiently distinguished thermodynamically stable from unstable compositions, also identifying their hybrid and inorganic family of perovskites with bandgaps in the desired range for usage in top and bottom layer in tandem structure [48]. This example shows that how a ML model can extrapolate chemical space using physical features at a fraction of computational cost of full DFT calculations.

There is a competing interplay between architecture of ML model and prediction accuracy when dealing with complex perovskite families. This challenge has been shown in the accelerated discovery review by Kumar *et al.* They showed that combining ML with automated synthesis and high throughput characterization can significantly accelerate the experimental discovery cycle. The review highlighted that ML models must account for synthesis dependent microstructure and processing induced nature of phases. These are the properties that are not captured by the descriptors of stable phases. Incorporating such features guide experimental design better [46].

ML for defect passivation

An ML workflow was developed by Huang *et al.* that specifically screens passivation candidates of small sized molecules for P-I-N perovskite solar cells. This implementation of ML can be considered beyond previously discussed prediction and design applications of ML. The authors used molecular descriptors obtained from known passivation chemistry and data available for device performance for training. The output of this ML model ranked the passivation molecules by their effectiveness. At the top lied ITIC (3,9-bis(2-methylene-(3-(1,1-dicyanomethylene)-indanone))-5,5,11,11-tetrakis(4-hexylphenyl)-dithieno[2,3-d:2′,3′-d′]-s-indaceno[1,2-b:5,6-b′] dithiophene) which was also validated experimentally. ITIC -passivated devices performed visibly better as the interfacial trap densities were measured to be reduced along with better charge extraction. This resulted in higher V_{OC} and filling factor (FF) [23]. This approach is using the chemical design rules that the defect passivation studies over the years have built with experiments. It says that effective passivation depends on Lewis acid base coordination, the ability to form hydrogen bonds and choosing functional groups which target specific defects [17,18,49]. Du *et al.* converts the design rules into quantitative screening criteria which enables pre-filtering of candidate molecules computationally instead of empirical approach. Only the most promising candidates will be then taken for experimental verification. Here we can conclude that the ML-passivation technique is not a replacement for defect chemistry but complements it and speeds up the process of selection [18].

Device simulation to connect material properties and actual device performance

Drift-diffusion simulation method provides a physics-based approach to relate material properties and performance of solar cell device made from it. This method utilizes defect density, layer thickness, doping concentration and energy level alignment as input parameters and study their effects on the device performance. A simulation at device level helps us know how some properties of materials effect the photovoltaic parameters. A recent study used drift-diffusion modelling to study inorganic hole transport layer (HTL) called $SrCu_2O_2$ on $FAPbI_3$. They varied the above-mentioned parameters to identify the conditions that resulted in PCE of 26.48%, V_{OC} = 1.25 V, J_{SC} = 23.51 mA cm^{-2} and FF = 89.5%. This gave us an understanding that with suitable band alignment at HTL and controlling defects in the absorber can push the device toward performing at Shockley-Queisser limit [45]. Such simulations help us design experiments for forming interfaces and synthesizing materials. Apart from that, researchers can implement the simulations to select suitable transport layers and conditions for interfaces before fabrication which reduces time and cost of experimentation. Hence, these simulation methods act actually as a bridge between knowing properties from computational or machine learning methods and performance of devices in experiments.

At the end, we find that DFT and ML are mostly complementary rather than competing approaches in the field of hybrid perovskite research. The experimental studies revealed the performance limits and operating conditions, while the first principles explained those trends

at the atomistic level through band-edge composition, defect analysis, ion migration and thermodynamic metastability of the photoactive phase of $FAPbI_3$. Based on these insights, ML models use descriptors like tolerance factor, ionic radii, electronegativity, formation energy and device architecture to accelerate composition screening, identifying passivation molecules and predict properties that would be too costly to do through only first principles. Besides those, we also find some discrepancies among these approaches. DFT usually reproduces the trends in bandgaps, phase stability and electronic structure, but often fails to fully capture processing-dependent disorder, defects, grain boundary chemistry and long-term environmental degradation. This happens as DFT often deals with the atomistic scale. The experimental studies include these effects but often report system specific outcomes and are difficult to generalize across different fabrication process and architectures of devices. This is due to it deals with limited type of material bulk. Dealing with many types for generalization becomes too costly. ML partly bridges this gap by learning from large DFT and experimental datasets, but sometimes predicts poorly when

Table 3: Comparison of experimental, DFT and ML findings for hybrid organic-inorganic perovskites.

Topic	Experimental	DFT / computational	ML	Remarks
$FAPbI_3$ stability & efficiency Ref: [3,6,9–13,20-22,41,45,46,49–51]	High-PCE α-$FAPbI_3$ devices; α→δ transition addressed by additives, 2D layers and mixed cations	Band edges, SOC bandgap reduction, α-phase metastability	Uses composition/stability datasets; FA-rich, optimized-t compositions are favorable.	All methods agree α-$FAPbI_3$ is electronically ideal but structurally fragile.
$MAPbI_3$ vs $FAPbI_3$ Ref: [3,6,9,20-22,41,45,46,48]	$FAPbI_3$ gives lower Eg and higher J_{SC} but needs stronger stabilization than $MAPbI_3$	Confirms narrower Eg and favorable band alignment of $FAPbI_3$ compared to $MAPbI_3$	Learns composition–E_g/stability trends, favoring FA-rich/mixed A-site systems.	FA-based systems are intrinsically superior but harder to stabilize.
Mixed A-site and X-site compositions Ref: [5,8,10 ,36,38–40,46–48.]	Mixed-cation/halide films tune t, suppress δ-phase and support efficient single-junction/tandem cells.	Shows mixed-cation/metal systems achieving suitable tolerance factor t, direct E_g and thermodynamic stability	Screening of large composition spaces via simple structural descriptors.	Compositional engineering is common to all; microstructure effects remain under-explored.
Defects & passivation Ref: [4, 20, 22, 23, 48, 50].	Identifies GBs/interfaces as main recombination sites; passivation and 2D interlayers reduce traps and boost V_{oc}/FF/stability.	Clarifies shallow/deep defects, migration barriers and passivator molecules	Screens passivation and interface molecules using chemistry-based descriptors.	All agree that multi-scale defect/interface control is critical for durable PCE.
2D/3D heterostructures Ref: [9,10,14–16,46-48.]	Thin 2D layers and localized 2D/3D junctions enhance moisture/thermal stability with modest transport penalty.	Links reduced dimensionality to stronger confinement, modified excitons and altered transport	Current models rarely encode explicit 2D/3D interface geometry or local strain.	2D/3D design is widely validated; proper descriptors for ML are yet to develop.
ML frameworks & applications Ref: [5,8,10 ,36,38–40,46–48.]	Reports efficient LEDs, detectors and tandems using similar structural/defect strategies as PV cells.	Provides band-edge/defect insights transferable to emission and detection problems	General ML tools for E_g, stability and PCE ready to extend to emission and detection metrics.	Same structure–property ideas extend beyond solar cells; ML method is the most used one for PCE.

data contain poorly described structures, and other effects due to synthesis process. Therefore, the disagreement in recent literature is not on the findings, but is on the scale a which each method deals with the material. Table 3 provides a summary of comparison of the approaches discussed previously.

Open challenges and outlook on the methods

The computational and ML methods reviewed in this section reveals that they form a coherent and a hierarchical approach for hybrid perovskite design. DFT calculations establish accurate and physics based relation between structure and properties at the base level [1,2]. The results from DFT methods are fed as inputs and physics based descriptors into ML models for selection of promising compositions [20,46–48] and passivation [23]. Simulations at device level relate the optimized material parameters to the device performance [45]. Although such developments are made, some challenges appear. The current ML models mostly work at the composition of the bulk or device, but the performance and stability of the devices are actually governed by defects like grain boundary, surface states, traps at interfaces etc. These require structural data beyond the information of a unit cell. Integrating these require DFT supercell calculations, impedance spectroscopy and the like to obtain proper physical descriptors to use as ML training data. This again demand high resource usage and thus remains a big challenge.

Conclusions

This review aspires to provide clarity on the choice of $FAPbI_3$ as a photovoltaic perovskite. The features like close to ideal bandgap for a single junction PV material, carrier lifetime, absorption across the visible spectrum, as suggested by Wang *et al.* [1], makes this an excellent candidate. The issue was regarding the stable phase. The α-phase has all the required photovoltaic property but the ground state happens to be the δ-phase, which is optically inert. After covering this, the review looks forward to a path and includes literature to draw a solution in order to prevent the transition as that would make $FAPbI_3$ an uninteresting material. Experiment based literature has provided us with a glimpse to achieve this. They mention layering of 2D perovskites on the 3D bulk [9,10,39]. Alongside layering we found that the researchers could manipulate the phase formation while crystallization takes place [50,51], engineer the chemical properties at grain boundaries and surface. These approaches basically address the common challenge of either avoiding or slowing down the conversion from α to δ phase and reducing the defects. A question then remains unanswered, that is, could the researchers converge at a common route to meet the challenges or many ways exist. But, the physics behind the working of perovskite solar cells has become clearer [17,18]. As an important step , ML as proved to be a useful accelerator in case of screening composition and passivation [23,47,48]. The challenges faced by ML also revealed that what could not be done yet. For crystals and known compositions, ML performs well. In case of processed films, which is available in real life, has messy data and the ML models have not performed well. The importance of grain boundaries, impurities, and processing history are to be given the same weight as that of chemical composition and stoichiometry [20,46]. This revelation also throws some light onto the future works in this research area. Overall, the literature show that the next considerable improvement in hybrid perovskite solar cells will not be gained from fixing just one issue, but from tackling phase stability, defects and the effects of processing together. The future research must aim beyond simply screening compositions and consider defects, grain boundaries and material's behavior in real operating conditions. Such kind of combined approach can help one design perovskite solar cells that are both highly efficient and stable enough for practical use.

References

1. Wang, S., Xiao, W. and Wang, F. 2020. Structural, electronic, and optical properties of cubic formamidinium lead iodide perovskite: a first-principles investigation. *RSC Advances*. **10**: 32364–32369. Doi: https://doi.org/10.1039/D0RA06028C
2. Wei, Q., Zi, W., Yang, Z. and Yang, D. 2018. Photoelectric performance and stability comparison of mapbi₃ and fapbi₃ perovskite solar cells. *Solar Energy*. **174**: 933–939. Doi: https://doi.org/10.1016/j.solener.2018.09.057
3. Masi, S., Echeverría-Arrondo, C., Muhammed Salim, K. M., Ngo, T. T., Méndez, P. F., López-Fraguas, E., Macias-Pinilla, D. F., Planelles, J., Climente, J. I. and Mora-Seró, I. 2020. Chemi-structural stabilization of formamidinium lead iodide perovskite by using g

embedded quantum dots. *ACS Energy Letters*. **5**(2): 418–427.
Doi: https://doi.org/10.1021/acsenergylett.9b02450

4. Mazumdar, S., Zhao, Y. and Zhang, X. 2021. Stability of perovskite solar cells: degradation mechanisms and remedies. *Frontiers in Electronics*. **2**: 712785.
Doi: https://doi.org/10.3389/felec.2021.712785
5. Verma, Tripathy ., et al. 2025. Toward stable and efficient mixed-cation mixed-halide perovskite solar cells. *IJESE*.
Doi: https://doi.org/10.35940/ijese.L2625.13121125
6. Zheng, Z., Wang, S., Hu, Y., Rong, Y., Mei, A. and Han, H. 2022. Development of formamidinium lead iodide-based perovskite solar cells: efficiency and stability. *Chemical Science*. **13**: 2167–2183.
Doi: https://doi.org/10.1039/D1SC04769H
7. Wang, Y., Zhang, X., Shi, Z., Zhang, L., Yu, A., Zhan, Y. and Ding, L. 2022. Stabilizing α-phase $fapbi_3$ solar cells. *Journal of Semiconductors*. **43**(4): 040202.
Doi: https://doi.org/10.1088/1674-4926/43/4/040202.
8. Byranvand, M. M., Otero-Martínez, C., Ye, J., Zuo, W., Manna, L., Saliba, M., Hoye, R. L. Z. and Polavarapu, L. 2022. Recent progress in mixed a-site cation halide perovskite thin-films and nanocrystals for solar cells and light-emitting diodes. *Advanced Optical Materials*. **10**(14): 2200423 .
Doi: https://doi.org/10.1002/adom.202200423
9. Liu, Y., Akin, S., Hinderhofer, A., Eickemeyer, F. T., Zhu, H., Seo, J.-Y., Zhang, J., Schreiber, F., Zhang, H., Zakeeruddin, S. M., Hagfeldt, A., Dar, M. I. and Grätzel, M. 2020. Stabilization of highly efficient and stable phase-pure $fapbi_3$ perovskite solar cells by molecularly tailored 2d-overlayers. *Angewandte Chemie International Edition*. **59**(36): 15688–15694.
Doi: https://doi.org/10.1002/anie.202005211
10. Hu, R., Zhang, Y., Paek, S., Gao, X.-X., Li, X. and Nazeeruddin, M. K. 2020. Enhanced stability of alpha-phase $fapbi_3$ perovskite solar cells by insertion of 2d $(pea)_2pbi_4$ nanosheets. *Journal of Materials Chemistry A*. **8**(16): 8058–8064.
Doi: https://doi.org/10.1039/C9TA14207J
11. Chen, M., et al. 2024. “Freezing” intermediate phases for efficient and stable fapbi 3 perovskite solar cells. *Energy & Environmental Science*. **17**(10): 3375–3383.
Doi: https://doi.org/10.1039/d4ee00865k
12. He, Q., et al. 2025. A self-assembled molecule directs ordered alpha-fapbi3 for n-i-p perovskite solar cells. *Nature Communications*.
Doi: https://doi.org/10.1038/s41467-025-68214-1
13. Kumar, A., et al. 2024. Superior stabilized α-fapbi3 perovskite solar cells with efficiency exceeding 24%. *Organic Electronics*. **135**: 107143.
Doi: https://doi.org/10.1016/j.orgel.2024.107143
14. Kim, E.-B., Akhtar, M. S., Shin, H.-S., Ameen, S. and Nazeeruddin, M. K. 2021. A review on two-dimensional (2d) and 2d–3d multidimensional perovskite solar cells: perovskites structures, stability, and photovoltaic performances. *Journal of Photochemistry and Photobiology C: Photochemistry Reviews*. **48**: 100405.
Doi:https://doi.org/10.1016/j.jphotochemrev.2021.100405.
15. Liu, D,. et al. 2025. Strain relaxation in halide perovskites via 2d/3d perovskite heterojunction formation. *Science Advances*.
Doi: https://doi.org/10.1126/sciadv.adu3459.
16. Zhao, X., et al. 2025. Exploring 2d perovskite chemistry for advancing efficient and stable solar cells. *Front. Energy*.
Doi: https://doi.org/10.1007/s11708-025-0997-1.
17. Gao, F., Zhao, Y., Zhang, X. and You, J. 2020. Recent progresses on defect passivation toward efficient perovskite solar cells. *Advanced Energy Materials*. **10**(9): 1902650
Doi: https://doi.org/10.1002/aenm.201902650.
18. Du, B., He, K., Zhao, X. and Li, B. 2023. Defect passivation scheme toward high-performance halide perovskite solar cells. *Polymers*. **15**(9): 2010.
Doi: https://doi.org/10.3390/polym15092010.
19. Li, Y., Wu, H., Qi, W., Zhou, X., Li, J., Shi, J., Wu, H., Luo, Y., Li, D. and Meng, Q. 2020. Passivation of defects in perovskite solar cell: from a chemistry point of view. *Nano Energy*. **78**: 105237
Doi: https://doi.org/10.1016/j.nanoen.2020.105237.
20. Tao, Q., Xu, P., Li, M. and Lu, W. 2021. Machine learning for perovskite materials design and discovery. *npj Computational Materials*. **7**: 23
Doi: https://doi.org/10.1038/s41524-021-00495-8.
21. Sa, R., Liu, D., Chen, Y. and Ying, S. 2020. Mixed-cation mixed-metal halide perovskites for photovoltaic applications: a theoretical study. *ACS Omega*. **5**: 4347–4351.
Doi: https://doi.org/10.1021/acsomega.9b04484.
22. Chen, J., Xu, W. and Zhang, R. 2022. Δ-machine learning-driven discovery of double hybrid organic–inorganic perovskites for photovoltaic applications. *Journal of Materials Chemistry A*. **10**: 1402–1413
Doi: https://doi.org/10.1039/D1TA09911F.
23. Huang, D., Guo, C., Li, Z., Zhou, H., Zhao, X., Feng, Z., Zhang, R., Liu, M., Liang, J., Zhao, L. and Meng, J. 2023. Machine learning-assisted screening of effective passivation materials for p–i–n type perovskite solar cells. *Journal of Materials Chemistry C: Materials for Optical and Electronic Devices*. **11**: 9602–9610
Doi: https://doi.org/10.1039/D3TC01140B.
24. Chin, S. 2025. Graph neural network based macroscale ai model for perovskite solar cell power conversion efficiency prediction. *European Journal of Energy Research*. **5**(3): 7–14
Doi: https://doi.org/10.24018/ejenergy.2025.5.3.7154.
25. Wang, J., et al. 2025. Exposing binding-favourable facets of perovskites for tandem solar cells. *Energy & Environmental Science*. **18**(15): 7680–7694
Doi: https://doi.org/10.1039/d5ee02462e.
26. Tyagi, V., Pols, M., Brocks, G. and Tao, S. 2025. Tracing ion migration in halide perovskites with machine learned force fields. *The Journal of Physical Chemistry Letters*.
Doi: https://doi.org/10.1021/acs.jpclett.5c01139.
27. de la Asunción-Nadal, V., Sprague, C. I., Guijarro-Berdiñas, B., Cappel, U. B. and García-Fernández, A. 2025. Machine learning for perovskite solar cells: a comprehensive review on opportunities and challenges for materials scientists. *EES Solar*.

Doi: https://doi.org/10.1039/d5el00041f.

28. Gong, J., Schneider, L. and Liu, Y. 2026. Review on perovskite solar cells: from single-junction devices to tandem deployment in space. *Advanced Sustainable Systems*. **10**(1): e01343
Doi: https://doi.org/10.1002/adsu.202501343.
29. Miah, M. H., Rahman, M. B., Nur-E-Alam, M., Islam, M. A., Shahinuzzaman, M., Rahman, M. R., Ullah, M. H. and Khandaker, M. U. 2025. Key degradation mechanisms of perovskite solar cells and strategies for enhanced stability: issues and prospects. *RSC Advances*. **15**(1): 628–654
Doi: https://doi.org/10.1039/d4ra07942f.
30. Sadia, H., Hasan, S. A. U., Rehan, S., Ali, I., Siddiqui, L., Abbas, R., Sidique, Y. and Kwak, S. K. 2025. Progress, current challenges, and future opportunities for sn-based perovskite solar cells: a comprehensive review. *Nano Energy*. **111627**
Doi: https://doi.org/10.1016/j.nanoen.2025.111627.
31. Dutta, S., Fransson, E., Hainer, T., Gallant, B. M., Kubicki, D. J., Erhart, P. and Wiktor, J. 2025. Revealing the low-temperature phase of fapbi3 using a machine-learned potential. *Journal of the American Chemical Society*. **147**(41): 37019–37029
Doi: https://doi.org/10.1021/jacs.5c05265.
32. Zhao, K., et al. 2025. Mitigating residual ma+ for stable fapbi3 perovskite photovoltaics. *Nature Communications*.
Doi: https://doi.org/10.1038/s41467-025-65045-y.
33. Jiang, S., et al. 2026. Multi-dimensional regulation toward fapbi3 crystal growth layer and passivation defects for efficient perovskite solar cells. *Nano Energy*.**111693**
Doi: https://doi.org/10.1016/j.nanoen.2025.111693.
34. Li, C., et al. 2026. Heterointeraction-induced nucleation promoting vertical growth and suppressing phase separation for efficient wide-bandgap perovskite solar cells and tandem devices. *Research; a journal of science and its applications*.
Doi: https://doi.org/10.34133/research.0892.
35. Fan, G.-F., Peng, L.-L., Jia, X.-H., Zuo, L.-H., Yan, J.-C., Chen, J.-Y., Hong, W.-C., Umbarkar, A. J. and Hong, W.-C. 2026. Optimizing performance prediction of perovskite photovoltaic materials by statistical methods-intelligent calculation model. *CMES*.
Doi: https://doi.org/10.32604/cmes.2025.064997.
36. Scalon, L. & Vaynzof, Y. 2025. Multidimensional perovskite solar cells: what's next after 3d/2d?. *Advanced Energy Materials*. **15**(44): 2502686
Doi: https://doi.org/10.1002/aenm.202502686.
37. Thote, A. M., Jeon, I., Lee, J.-W., Seo, S., Lin, H.-S., Nakamura, S., Matsuo, Y., Yang, Y., Dawood, H. and Miyajima, S. 2019. Stable and reproducible 2d/3d formamidinium–lead–iodide perovskite solar cells. *ACS Applied Energy Materials*. **2**(4): 2486–2493.
Doi: https://doi.org/10.1021/acsaem.8b01964.
38. Zhang, Q., et al. 2025. Multifunctional butylammonium acetate additive regulates fapbi3 perovskite film crystallisation. *Advanced Functional Materials*.
Doi: https://doi.org/10.1002/adfm.202507934.
39. Huang, W., Bu, T., Huang, F. and Cheng, Y.-B. 2020. Stabilizing high efficiency perovskite solar cells with 3d–2d heterostructures. *Joule* **4**(5): 975–979.
Doi: https://doi.org/10.1016/j.joule.2020.04.009.
40. Ge, C., Xue, Y., Li, L., Tang, B. and Hu, H. 2020. Recent progress in 2d/3d multidimensional metal halide perovskites solar cells. *Frontiers in Materials*. **7**: 601179
Doi: https://doi.org/10.3389/fmats.2020.601179.
41. Kareem, S. H., Elewi, M. H., Naji, A. M., Ahmed, D. S. and Mohammed, M. K. A. 2022. Efficient and stable pure α-phase $fapbi_3$ perovskite solar cells with a dual engineering strategy: additive and dimensional engineering approaches. *Chemical Engineering Journal*. **443**: 136469
Doi: https://doi.org/10.1016/j.cej.2022.136469.
42. Chen, J., et al. 2026. Localized 2d/3d heterojunction enhances photovoltage for wide-bandgap perovskite solar cells. *Nature Communications*.
Doi: https://doi.org/10.1038/s41467-026-68904-4.
43. Lee, J., Moon, C. S., Kim, Y., Kim, Y. Y., Park, E. Y. and Yoo, J. J. 2026. Tailored n value engineering of dion-jacobson 2d layers enables efficient and stable perovskite solar cells. *Joule*. **10**(3)
Doi: https://doi.org/10.1016/j.joule.2025.102301.
44. Shen, X. et al., 2026. Key advancements and emerging trends of perovskite solar cells in 2024–2025. *Nano-Micro Letters*. **18**(1): 209
Doi: https://doi.org/10.1007/s40820-025-02022-6.
45. Noman, M., Shahzaib, M., Jan, S. T., Shah, S. N. and Khan, A. D. 2023. 26.48% efficient and stable $fapbi_3$ perovskite solar cells employing $srcu_2o_2$ as hole transport layer. *RSC Advances*. **13**: 1892–1905
Doi: https://doi.org/10.1039/D2RA06535E.
46. Kumar, S., Dutta, S., Jaafreh, R., Singh, N., Sharan, A., Hamad, K. and Yoon, D. H. 2023. Accelerated discovery of perovskite materials guided by machine learning techniques. *Materials Letters*. **353**: 135311
Doi: https://doi.org/10.1016/j.matlet.2023.135311.
47. Liu, Y., Tan, X., Liang, J., Han, H., Xiang, P. and Yan, W. 2023. Machine learning for perovskite solar cells and component materials: key technologies and prospects. *Advanced Functional Materials*. **33**.
Doi: https://doi.org/10.1002/adfm.202214271.
48. Chen, J., Feng, M., Zha, C., Shao, C., Zhang, L. and Wang, L. 2022. Machine learning-driven design of promising perovskites for photovoltaic applications: a review. *Surf. Interfaces*. **35**: 102470
Doi: https://doi.org/10.1016/j.surfin.2022.102470.
49. Zhao, K., et al. 2025. Mitigating residual ma+ for stable fapbi3 perovskite photovoltaics. *Nature Communications*.
Doi: https://doi.org/10.1038/s41467-025-65045-y.
50. Mandal, T. N., Heo, J. H., Im, S. H. and Kim, W.-S. 2023. Highly efficient and stable inverted perovskite solar cell using pure δ-$fapbi_3$ single crystals. *Small*. **19**(52): e2305246 .
Doi: https://doi.org/10.1002/smll.202305246.
51. Niu, T., Chao, L., Xia, Y., Wang, K., Ran, X., Huang, X. and Chen, Y. 2024. Phase-pure α-$fapbi_3$ perovskite solar cells via activating lead–iodine frameworks. *Advanced Materials*. **36**(13): 2309171.
Doi: https://doi.org/10.1002/adma.202309171.